ACS APPLIED MATERIALS & INTERFACES

Research Article

www.acsami.org

Assembly Modulation of PDI Derivative as a Supramolecular Fluorescence Switching Probe for Detection of Cationic Surfactant and Metal Ions in Aqueous Media

Atul K. Dwivedi,‡ M. Pandeeswar,‡ and T. Govindaraju*

Bioorganic Chemistry Laboratory, New Chemistry Unit, Jawaharlal Nehru Centre for Advanced Scientific Research, Jakkur P.O., Bengaluru 560064, India

Supporting Information

ABSTRACT: We report an amphiphilic perylene diimide (**1**), a bimolecular analog of L-3,4-dihydroxyphenylalanine (L-DOPA), as a reversible fluorescence switching probe for the detection and sensing of cationic surfactants and Fe^{3+}/Cu^{2+} in an aqueous media respectively by means of host–guest interactions driven assembly and disassembly of **1**. Photophysical studies of **1**, going from dimethyl sulfoxide (DMSO) (State-I) to pure aqueous medium (State-II), suggested the formation of self-assembled aggregates by displaying very weak fluorescence emission along with red shifted broad absorption bands. Interestingly, the cationic surfactant cetyltrimethylammonium bromide (CTAB) could disassemble **1** in micellar conditions by restoring bright yellow fluorescence and vibronically well-defined (Franck–Condon progressions $A_{0-0}/A_{0-1} \approx 1.6$) absorption bands of **1** over other neutral and anionic surfactants (State-III). Owing to the metal chelating nature of L-DOPA, **1** was able to sense Fe^{3+} and Cu^{2+} among a pool of other metal ions by means of fluorescence switching off state, attributed to metal interaction driven assembly of **1** (State-IV). Such metallosupramolecular assemblies were found to reverse back to the fluorescence switching on state using a metal ion chelator, diethylenetriaminepentaacetic acid (DTPA, State-III), further signifying the role of metal ions toward assembly of **1**. Formation of assembly and disassembly could be visualized by the diminished and increased yellow emission under green laser light. Further, the assembly–disassembly modulation of **1** has been extensively characterized using infrared (IR), mass spectrometry, microscopy and dynamic light scattering (DLS) techniques. Therefore, modulation of the molecular self-assembly of PDI derivative **1** in aqueous media (assembled state, State-II) by means of host–guest interactions provided by micellar structures of CTAB (disassembled state, State-III), metal ion (Fe^{3+} and Cu^{2+}) interactions (assembled state, State-IV) and metal ion sequestration using DTPA (disassembled state, State-III) is viewed as a supramolecular reversible fluorescence switching off–on probe for cationic surfactant CTAB and Fe^{3+}/Cu^{2+}.

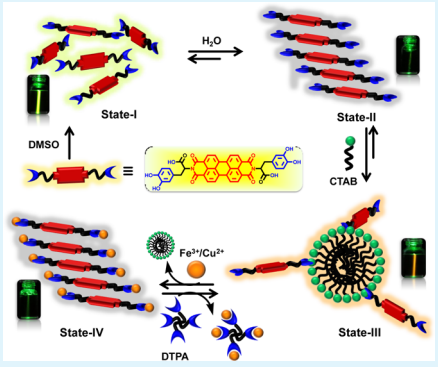

KEYWORDS: *assembly modulation, cationic surfactant, micellar media, fluorescence switching, metallosupramolecular aggregates*

1. INTRODUCTION

Over the past few years, molecular and supramolecular probes based on perylene diimide (PDI) derivatives in aqueous medium have attracted much attention because of their several advantageous properties such as thermal stability, chemical inertness, high tinctorial strength with a wide range of colors, photochemical stability and high fluorescence.[1−7] With such advantageous properties, PDI derivatives have been considered as optimal fluorescent dyes and utilized in a wide variety of applications such as laser dyes, photovoltaic cells, fluorescence switches, molecular wires, molecular transistors and sensors.[8−17] However, the PDI structure and planar π-electron deficient aromatic nature are known to promote strongly the formation of aggregates through stacking interactions between the π-conjugated core[1] and this strong aggregation tendency in aqueous media results in fluorescence quenching.[18,19] Inspite of aggregation and resultant low fluorescence, PDI derivatives have been considered to be excellent fluorophores in sensor design because of their excellent electron accepting ability and high fluorescence in the disassembled state.[20,21] Thus, recent years witnessed some efforts toward developing PDI derivatives based fluorescence sensors. In these reports, organic solvents along with some compositions of aqueous solutions were used to obtain PDI derivatives in the disassembled state. Moreover, limited reports are known to use PDI derivatives in only aqueous solution. To overcome the disadvantage owing to aggregation, aqueous solubility of PDI derivatives was improved by incorporating hydrophilic substituents at the diimide positions.[22−28] However, PDI derivatives with hydrophilic substituents such as carboxylic, sulfonic and other ionic functionalities generally show low fluorescence emission due to predominant π–π stacking and especially in case of ionic

Received: September 17, 2014
Accepted: November 18, 2014
Published: November 18, 2014

functionalities $\pi-\pi$ stacking was supposed to be removed by the complexation with oppositely charged moieties.[29] In all these reports, fluorescence sensing was supposed to be based on either the photoinduced electron transfer (PET) mechanism or assembly and disassembly of the PDI derivative.[21−23,5] However, the key daunting challenge of making PDI fluoresce under aqueous media remains to be addressed to further the advancement in PDI based molecular systems and materials for biological and environmental applications.

Detection of biologically important metal ions such as Fe^{3+} and Cu^{2+} has gained significant interest. Although these metal ions are essential for the proper functioning of all living cells, their excessive concentrations are detrimental and lead to various biological disorders.[31−35] In this context, biomolecules such as amino acids and their derivatives are particularly appealing due to their remarkable metal chelating nature, aqueous solubility, specific molecular recognition, and ability to self-assemble into functional, complex and highly ordered molecular systems and nanomaterials through various noncovalent interactions.[36−41] Herein we report an easy one-step synthesis of PDI derivative **1** with L-3,4-dihydroxyphenylalanine (L-DOPA) functionality as a well-known receptor at the N-imide positions, and assembly−disassembly modulated detection of Fe^{3+} and Cu^{2+} metal ions. It was presumed that incorporation of L-DOPA would render the aqueous solubility to PDI derivative **1** and, consequently, a fluorescence probe in aqueous medium could be established. However, synthesized PDI derivative **1** was found to be predominantly assembled in aqueous medium, as confirmed by weak fluorescence and characteristic absorption spectral features. We hypothesized that disassembly of **1** can be achieved in the micellar media of a cationic surfactant. Consequently, our investigations in the present study revealed a disassembly and a bright yellow fluorescence of **1** under laser light, in the presence of miceller aqueous media of the cationic surfactant cetyltrimethylammonium bromide (CTAB) over other neutral (Triton X 100) and anionic (sodium dodecyl sulfate (SDS)) surfactants. Moreover, such a bright yellow fluorescence of disassembled PDI could be quenched (aggregated state) by the selective interaction with metal ions (Fe^{3+} and Cu^{2+}), leading to formation of a complex between L-DOPA in **1** and metal ions. Furthermore, metal ions induced aggregated fluorescence switch off state of **1** could be reversed back into switch on yellow fluorescence (molecularly dissolved state) by sequestrating the metal ions (Fe^{3+} and Cu^{2+}) using a well-known metal ions chelator, diethylenetriaminepentaacetic acid (DTPA). Thus, a fluorescence "switching off−on" probe was established through modulation of assembly and disassembly of PDI derivative **1**. To the best of our knowledge, the present study represents the first example of the assembly−disassembly driven switching off−on fluorescence for the detection and sensing cationic surfactant and metal ions in aqueous medium, respectively. We propose our investigations could provide valuable insights to elucidate the role of host species toward assembly and disassembly of PDI derivatives.

2. EXPERIMENTAL SECTION

2.1. Reagents and Materials. 3,4,9,10-Perylenetetracarboxylic dianhydride (PDA), L-3,4-dihydroxyphenylalanine (L-DOPA) imidazole and all the perchlorate salts of metal ions were obtained from Sigma-Aldrich. All other reagents and solvents utilized in the experiments were of reagent and spectroscopic grades and used as received without further purification unless otherwise mentioned. Milli-Q water was used in all the experiments.

2.2. Measurements. UV−vis absorption and fluorescence emission spectra were recorded on a PerkinElmer Lambda-25 spectrometer. A 10 × 10 mm quartz cuvette was used for recording spectra of samples in solution. Fourier transform infrared (FTIR) spectra were recorded on a PerkinElmer spectrometer. ^{1}H and ^{13}C NMR spectra were recorded on a Bruker AV-400 spectrometer with chemical shifts reported as ppm (in DMSO-d_6 with tetramethylsilane as the internal standard). High resolution mass spectrometry (HRMS) analysis was performed on Agilent Technologies 6538 UHD Accurate-Mass Q-TOF liquid chromatography mass spectrometry (LC/MS) spectrometer (HRMS). Electrospray ionization mass spectrometry (ESI-MS) analysis was performed on a Shimadzu LCMS-2020 spectrometer. Fluorescence decay profiles were performed using a FLSP 920 spectrometer, Edinburgh Instrument, EPLED.

2.3. Synthesis of 1. 3,4,9,10-Perylenetetracarboxylic dianhydride (PDA) (500 mg, 1.2 mmol), L-3,4-dihydroxyphenylalanine (L-DOPA) (500 mg, 2.5 mmol) and imidazole (2.0 g) were added into a round-bottom flask, and the solution was heated at 120 °C for 1 h with stirring under a nitrogen atmosphere. The reaction mixture was allowed to cool to 90 °C, and then poured into Milli-Q water and filtered. The filtrate was acidified with 2.0 N HCl, and the precipitate was filtered, washed with excess of Milli-Q water and dried under vacuum at 40 °C to obtain the product **1** in high yield (94%). ^{1}H NMR (DMSO-d_6, 400 MHz) δ_H 13.01 (2H, s), 8.83 (2H, s), 8.56 (2H, s), 8.18−7.98 (8H, br), 6.71−6.58 (6H, m), 5.96 (2H, t), 3.49−3.37 (4H, m); ^{13}C NMR (DMSO-d_6, 100 MHz) δ_C 170.7, 162.1, 144.8, 143.7,133.2, 130.9, 128.3, 127.8, 124.8, 123.0, 121.6, 119.8, 116.4, 115.3, 53.7, 33.5. HR-MS: m/z found 751.1563 $[M + H]^+$; calcd. 750.1486 for $C_{42}H_{26}N_2O_{12}$.

3. RESULTS AND DISCUSSION

We report the use of synthesized amphiphilic PDI derivative **1** with L-DOPA functionality at the N-imide positions as fluorescence switch off−on probe for cationic surfactant and metal ions (Scheme 1). In a series of investigations to explore the photophysical properties of **1**, we recorded absorption and fluorescence spectra in dimethyl sulfoxide (DMSO) and water (Figure 1). The absorption spectrum in DMSO solution showed well-resolved vibronic absorption bands centered at 522 nm (0−0 transition) along with three higher electronic

Scheme 1. Synthesis of L-DOPA Conjugated PDI Derivative 1

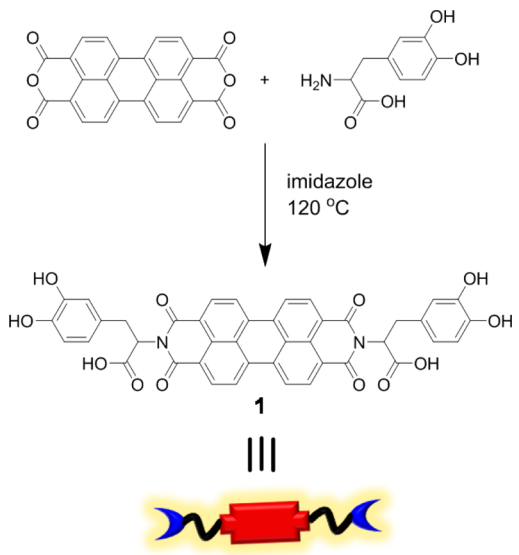

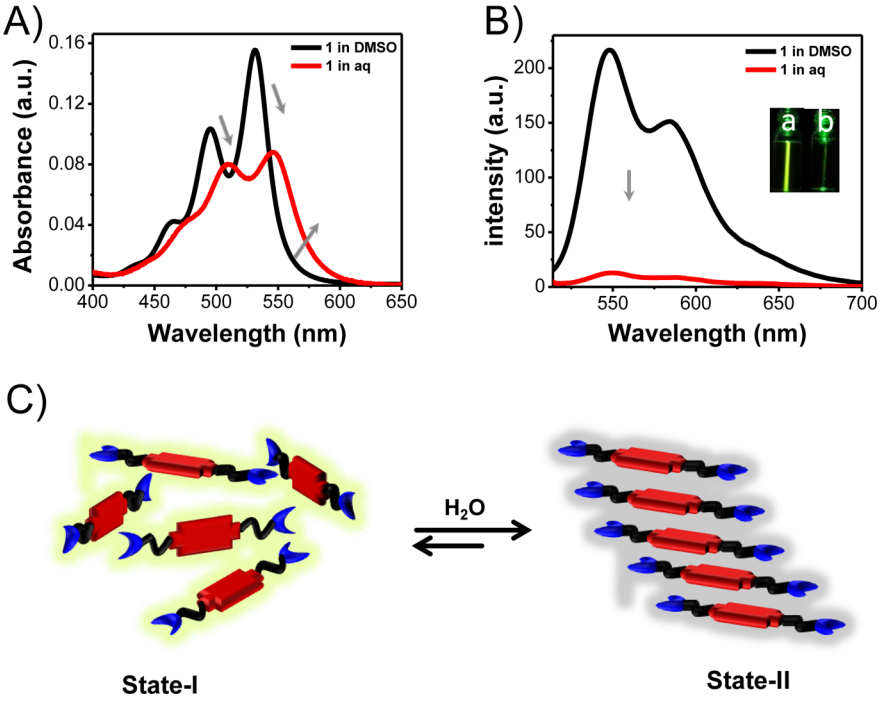

Figure 1. UV−vis absorption (A) and fluorescence emission spectra (B) of **1** (3.5 μM) in DMSO and water. Inset: solutions of **1** in DMSO (a) and water (b) under green laser light. (C) Schematic representation of molecular organization of **1** in DMSO (molecularly dissolved State-I) and in aqueous solution (aggregated State-II).

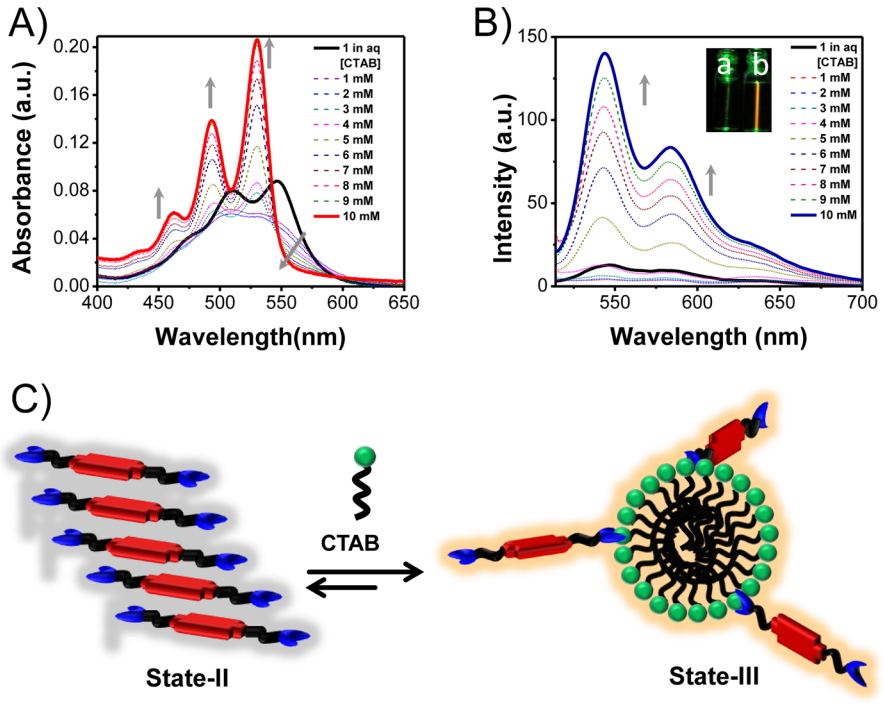

Figure 2. UV−vis absorption (A) and fluorescence emission spectra (B) of **1** (3.5 μM) in water with increase in concentration of CTAB. Inset: solutions of **1** in water (a) and in CTAB miceller media (b) under green laser light. (C) Schematic representation of transformation of aggregated State-II of **1** to molecularly dissolved State-III in the presence of CTAB micelles.

excitation states at 485 nm (0−1 transition), 454 nm (0−2 transition) and 425 nm (0−3 transition), which are assigned to the typical absorption spectrum of the molecularly dissolved state of **1** (Figure 1A).[29] The corresponding fluorescence emission studies further confirmed the absence of any assembled state by displaying mirror image emission spectrum with the E_{max} at 545 nm. The yellow fluorescence, as a consequence of molecularly dissolved state of **1**, can be visualized under green laser light (Figure 1B, State-I in Figure 1C).

It has been established in previous reports that the absorption intensity ratio of the 0−0 and 0−1 transitions

dx.doi.org/10.1021/am5063844 | ACS Appl. Mater. Interfaces 2014, 6, 21369−21379

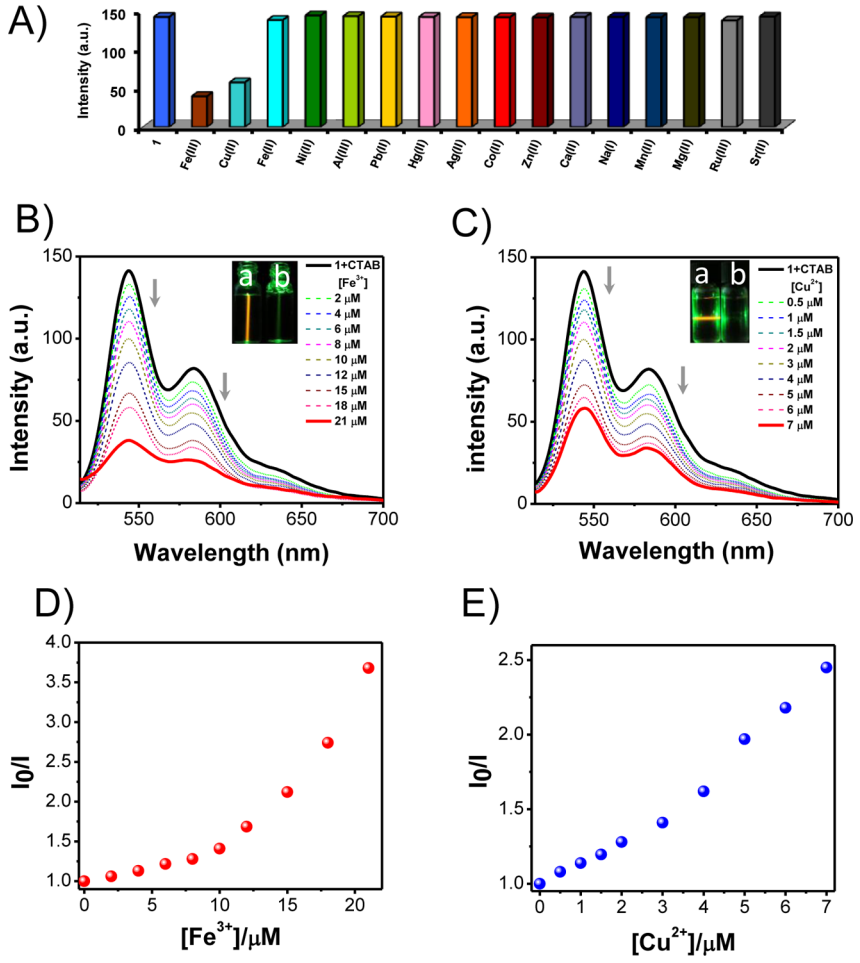

Figure 3. Fluorescence response of **1** (3.5 μM) in the micelle media of CTAB (10 mM) solution. (A) Bar diagram depicting the effect of various metals ions on the fluorescence intensity of **1** (3.5 μM). (B) Fluorescence emission spectra of **1** (3.5 μM) with increasing concentration of Fe^{3+} shows 3.5-fold quenching in aqueous solution. Inset: solutions of **1** in the absence (a) and presence (b) of Fe^{3+} in the CTAB micelle media under green laser light. (C) Fluorescence emission spectra of **1** (3.5 μM) in the presence of increasing concentration of Cu^{2+} in aqueous media. Inset: solutions of **1** under green laser light in the absence (a) and presence (b) of Cu^{2+}. (D,E) Plots of fluorescence response (I_0/I) of **1** versus concentration of added Fe^{3+} and Cu^{2+}, respectively.

(A_{0-0}/A_{0-1}) can be utilized as an indicator of the degree of aggregation of the PDI derivatives.[1,3,6,9,12,15−41] The calculated ratio was reported to be 1.59 for the disassembled PDI. The absorption spectrum of **1** (3.5 μM) in pure water was found to be broad structured, attributed to predominantly the assembled state (Figure 1A). This led to a significant fluorescence quenching of **1** in pure water as visualized under green laser light (Figure 1B, inset). The absorption intensity observed for the 0−0 band was found to be still higher than that for the 0−1 band (A_{0-0}/A_{0-1}, Franck−Condon value = 1.1), indicating a favorable Franck−Condon factor for the (0−0) excited state and thus suggesting the formation of J-type $\pi-\pi$ stacking assembly in aqueous solution (State-II, Figure 1C). The assembled state of **1** in water was further confirmed by concentration dependent emission spectra from 0 to 3.5 μM. The fluorescence intensity decreased as a function of increased concentration of **1** and the trend reached saturation at 3.5 μM. Moreover, the decrease in fluorescence may be attributed to intermolecular $\pi-\pi$ stacking, which is postulated to play a significant role in controlling the emissive properties of PDI fluorophore. Therefore, intermolecular interactions at higher concentrations were solely responsible for self-quenching of **1**. Furthermore, changes in fluorescence response of **1** at concentrations >3.5 μM were found to be insignificant in the presence of various cationic, anionic and neutral species.

To examine whether or not self-assembled PDI **1** could be used as a probe to detect targeted analytes, initial spectroscopic behavior was investigated in the miceller media of cationic, neutral and anionic surfactants such as CTAB, Triton X 100 and SDS. It is evident from previous reports that surfactants above their critical micelle concentration (CMC) can solubilize even hydrophobic species in water, and could break up aggregates formed by the intermolecular hydrophobic interactions.[18] With this concept in mind, changes in photophysical properties of **1** were monitored by performing the controlled experiments in the absence and presence of cationic (CTAB), neutral (Triton X 100) and anionic (SDS) surfactants in aqueous media (Figure 2). Eleven samples, with increasing concentrations of surfactants (0, 1, 2, 3, 4, 5, 6, 7, 8, 9 and 10 mM) were added to a fixed concentration of **1** (3.5 μM), and the changes in the photophysical properties were recorded. **1** in the presence of lower concentrations of aqueous CTAB (0 to 1.98 mM) did not exhibit significant changes in the fluorescence as well as absorption intensities due to aggregates, as shown in Figure 2A,B. This is presumably due to the formation of nonfluorescent premicellar aggregates as a result

dx.doi.org/10.1021/am5063844 | ACS Appl. Mater. Interfaces 2014, 6, 21369−21379

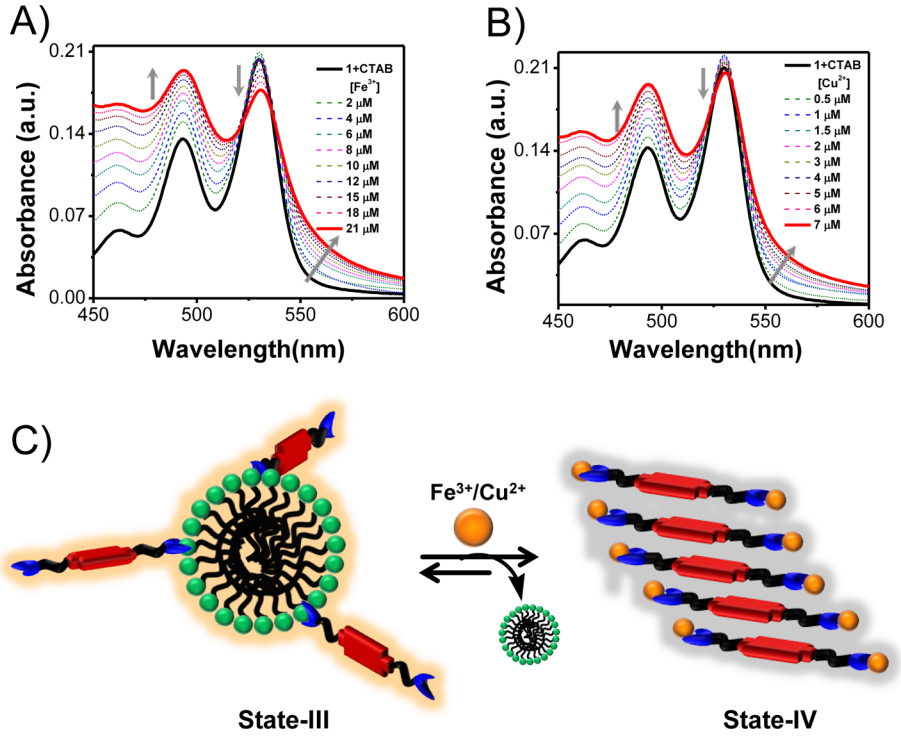

Figure 4. UV−vis absorption spectra of **1** (3.5 μM) with increasing concentrations of Fe^{3+} (A) and Cu^{2+} (B). (C) Schematic representation of transformation of State-III to State-IV via metal ion induced reorganization of 1 in the presence of CTAB micelles.

of electrostatic interactions between aggregates of **1** and CTAB. Whereas further addition of CTAB from 2 to 10 mM induced dramatic changes in absorption as well as fluorescence intensities of **1**. The absorption spectrum of **1** at higher CTAB concentration (10 mM) displayed a 15 nm blue shift along with the well-resolved vibronic absorption bands at 530, 492, 460 and 430 nm, corresponding to 0−0, 0−1, 0−2 and 0−3 transitions, respectively.[42] Employing the reported method, we calculated the ratio of absorption intensities of 0−0 to 0−1 transitions and found to be around 1.51, which is almost equal to the normal Franck−Condon progressions ($A_{0-0}/A_{0-1} \approx 1.6$) for the free PDI molecules.[43] Corresponding fluorescence emission spectra exhibited a steady increase of almost 12-fold in the fluorescence intensity of **1** and reached a plateau at 10 mM concentration of CTAB, as shown in Figure 2B. A rapid fluorescence response (within 1 min) was observed after each consecutive addition of CTAB and the emission intensity was saturated at above 10 mM CTAB. The fluorescence switching off−on (assembly and disassembly respectively) process of **1** could be visualized by the naked eye under green laser light, as shown in Figure 2B inset. To ascertain the selectivity of cationic surfactant CTAB toward disassembly of **1**, we further carried out similar experiments with neutral (Triton X100) and anionic (SDS) surfactants. The photophysical studies of **1** revealed limited absorption and fluorescence emission changes over the investigated concentration range in the presence of Triton X100 and SDS. These studies confirmed that only cationic surfactant CTAB micellar medium could able to disassemble the intermolecular $\pi-\pi$ stacking interactions of PDI **1** into molecularly dissolved State-III through complementary electrostatic interactions between L-DOPA of **1** and CTAB, which, subsequently, led to fluorescence emission with E_{max} at 545 nm (Figure 2C). This study also emphasized the utility of assembled state of **1** as a selective supramolecular fluorescent probe for the cationic surfactant (CTAB).

The pendant L-DOPA functional group is a known receptor and assumed to facilitate the binding events with metal ions. We hypothesized that the metal ions may disrupt the electrostatic interactions present in CTAB micellar bound **1** via a strong metal chelating interaction that results in metallosupramolecular aggregates.[43] Various alkali as well as transition metal perchlorate ions were chosen to study the selectivity, change in optical properties and probable metal chelation driven reorganization of **1** in the miceller media of CTAB solution. Our preliminary investigations based on the changes in fluorescence emission of **1** in the presence of various metal ions are shown in Figure 3. The fluorescence emission of **1** in the miceller media of CTAB was almost unaffected upon excitation at 490 nm in the presence of most of the alkali and transition metal ions (Fe^{2+}, Ni^{2+}, Al^{3+}, Pb^{2+}, Hg^{2+}, Ag^{+}, Co^{2+}, Zn^{2+}, Ca^{2+}, Na^{+}, Mn^{2+}, Mg^{2+}, Ru^{3+} and Sr^{2+}) even at their 25 μM concentrations (Figure 3A). However, addition of Fe^{3+} and Cu^{2+} quenched the fluorescence of **1** in the micellar media of CTAB in aqueous solution. With increasing concentration of metal ions ranging from 0 to 21 μM (Fe^{3+}) and 0 to 7 μM (Cu^{2+}) respectively, significant fluorescence quenching was observed and leveled off due to the formation of larger nonemitting aggregates of metal bound **1** (Figure 3B,C). Moreover, the fluorescence quenching of **1** with Fe^{3+} and Cu^{2+} was found to be 3.5-fold and 2.5-fold, respectively, within the investigated concentration range. This change in fluorescence emission was also visualized by the diminished yellow emission color of **1** under green laser as shown in Figure 3B,C inset. The fluorescence quenching corresponds to metallosupramolecular aggregates (State IV) formed by the association of metal coordinated **1**. Figure 3D,E depicts the decreasing fluorescence intensity pattern of **1** in the presence of Fe^{3+} and Cu^{2+},

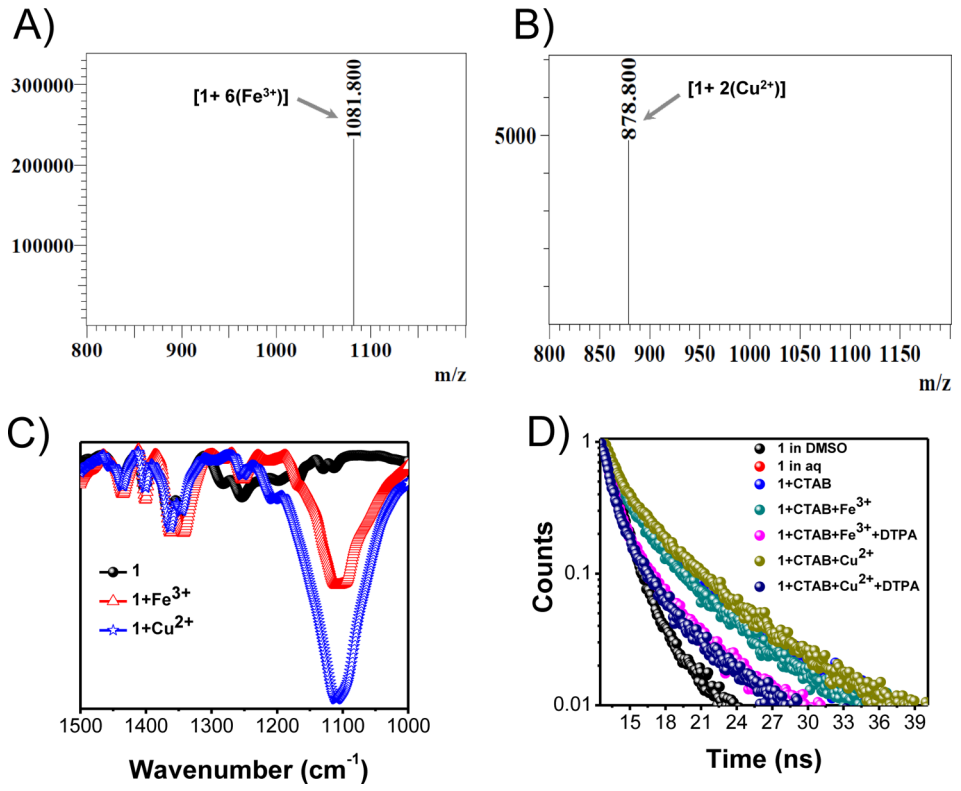

Figure 5. ESI-MS spectra of **1** in the presence of metal ions (A) Fe^{3+} and (B) Cu^{2+}. (C) FTIR spectra (C−O stretching frequency region 1500 to 1000 cm^{-1}) of **1** in absence and presence of Fe^{3+} and Cu^{2+}. (D) TCSPC decay profile of **1** (E_{max} = 545 nm) with a 500 nm excitation.

respectively. At lower concentrations of metal ions, fluorescence quenching behavior of **1** was found to be linear. However, at higher concentrations, linearity was lost and plot became nonlinear, indicating a static type of quenching. Furthermore, efficiencies of fluorescence quenching of **1** in the presence of metal ions were determined over the linear region of the plot by generating a Stern−Volmer plot, followed by a comparison.

$$I_0/I = 1 + K_{sv}[Q]$$

Where I_0 and I are fluorescence intensities in the absence and presence of the quencher, respectively, K_{sv} is the Stern−Volmer constant and the value of K_{sv} of an artificial assay indicates the sensitivity of the probe toward the analyte, and [Q] is the quencher concentration. K_{sv} values for **1** in the presence of Fe^{3+} and Cu^{2+} metal ions were found to be 4×10^4 and 1.35×10^5 M^{-1} respectively, as shown in Figure S5 (Supporting Information). The high K_{sv} values of **1** toward Cu^{2+} and Fe^{3+} further confirmed that PDI **1** is a selective and sensitive supramolecular probe for sensing of Cu^{2+} and Fe^{3+} in aqueous medium. Further, we explored the pH dependence on the sensing propensity of **1** toward Cu^{2+} and Fe^{3+} in CTAB aqueous media (Figure S6, Supporting Information). The sensing behavior of **1** in CTAB aqueous media toward Cu^{2+} and Fe^{3+} was found to be sensitive at lower (<2) and higher (>8) pH values. However, sensing of these metal ions (Cu^{2+} and Fe^{3+}) by **1** was unaffected in the normal pH range of 2−8.

After investigating the significant fluorescence quenching of **1**, we further examined changes in the absorption intensity of **1** in the presence of Fe^{3+} and Cu^{2+} in aqueous CTAB miceller conditions. Our observations revealed a broadened absorption spectrum of **1** (3.5 μM) with a decrease in absorption intensity at 530 nm (0−0 transition), whereas the 492 nm (0−1 transition) band was significantly increased and thus changed the ratio of 0−0 and 0−1 transition bands effectively, as shown in Figure 4A,B. However, higher concentrations of metal ions (>21 μM of Fe^{3+} and >7 μM of Cu^{2+}) were found to be not effective in further decreasing or increasing the intensity of the 0−0 or 0−1 transition bands, respectively. Thus, UV−vis absorption and fluorescence emission studies showed that **1** was in predominantly assembled state at the stoichiometric ratio (**1**: metal ion) of 1:6 with Fe^{3+} and 1:2 with Cu^{2+} in aqueous CTAB miceller conditions. Moreover, the observed absorption spectral features upon addition of Fe^{3+}/Cu^{2+} reflect a different kind of assembly behavior of **1**, as compared to assembly of **1** in water (State-II, Figure 1A). It is reported in the literature that the 0−0 and 0−1 bands in the absorption spectra of PDI decrease simultaneously while stacking.[44] However, the absorption spectrum of **1** revealed a decreased 0−0 band intensity and increased 0−1 band intensity simultaneously in the presence of Fe^{3+} and Cu^{2+} in aqueous miceller media (Figure 4A,B). We reason that metal ions play important role toward coordination with L-DOPA in **1** and thus facilitating the reorganization of **1** via metallosupramolecular aggregate formation (transformation of State-III to State-IV, Figure 4C).

Furthermore, complexation and stoichiometry between **1** and Fe^{3+}/Cu^{2+} was confirmed by electrospray ionization mass spectrometry (ESI-MS) studies in aqueous media (Figure 5A,B). Due to the high concentration of surfactant (CTAB) used in our experiments discussed above as compared to **1** and metal ion, mass spectrometry studies were performed without CTAB in pure water. The molecular-ion peak showed the formation of $[(\mathbf{1} - 4H^+) + 6(Fe^{3+})]$ [MW: found 1081.80; calcd. 1081.73 for $C_{42}H_{22}Fe_6N_2O_{12}$)] and $[(\mathbf{1} + H^+) + 2(Cu^{2+})]$ [MW: found 878.80; calcd 878.75 for

dx.doi.org/10.1021/am5063844 | ACS Appl. Mater. Interfaces 2014, 6, 21369−21379

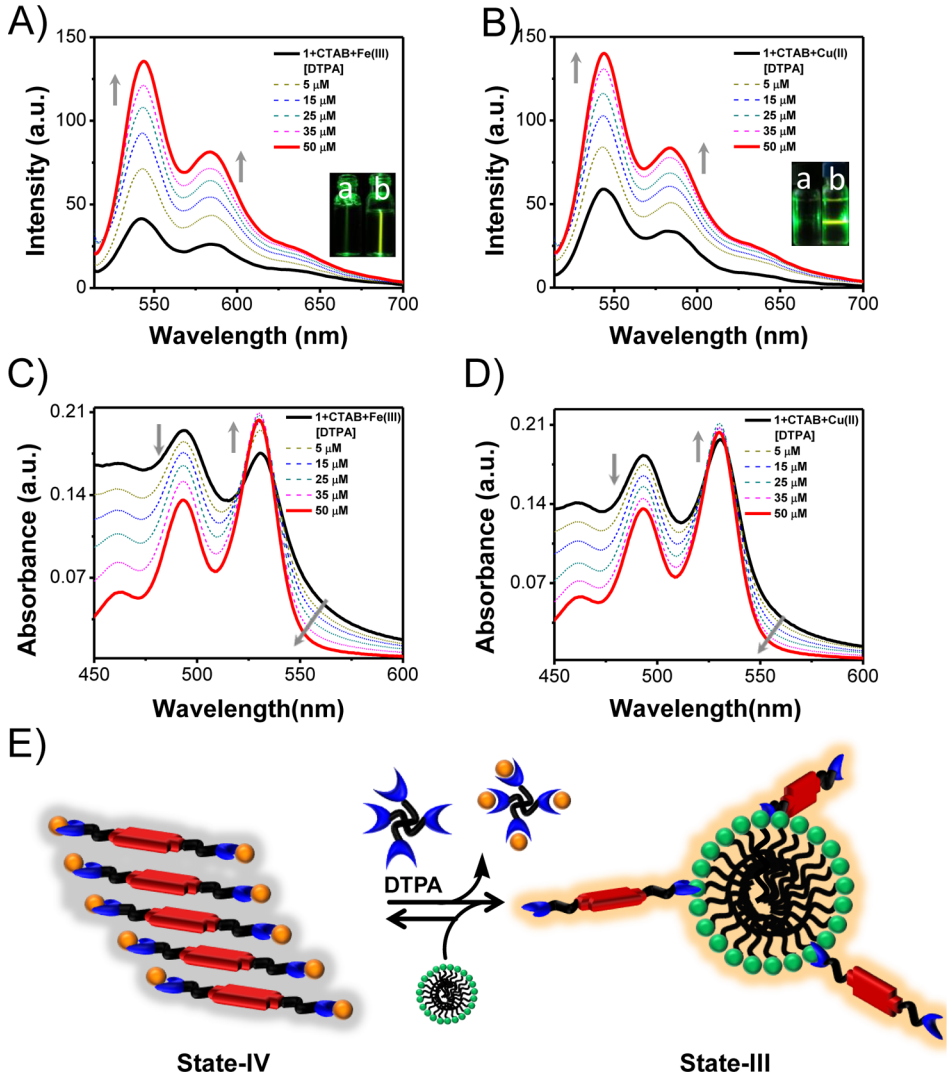

Figure 6. Fluorescence emission spectra (A and B) and UV−vis absorption spectra (C and D) of [**1**+CTAB+Fe^{3+}] and [**1**+CTAB+Cu^{2+}] solutions with increase in concentrations of DTPA in CTAB micellar aqueous medium. Inset: solutions of corresponding 1 under green laser light in the absence (a) and presence of DTPA (b). E) Schematic representation of sequestration of metal ion from metallosupramolecular aggregate (State-IV) using DTPA into molecularly dissolved state (State-III).

$C_{42}H_{27}Cu_2N_2O_{12}$)], respectively. Therefore, in agreement with photophysical studies mass analysis revealed the formation of matallosupramolecular aggregates with the stoichiometric compositions (**1**: metal ion) of 1:6 and 1:2 for Fe^{3+} and Cu^{2+}, respectively.

To determine the mode of metal chelation in **1**, we performed FTIR spectroscopy measurements of **1** with and without metal ions. Upon metal complexation the intense band at 1109 cm^{-1} was observed which was absent in **1** alone (Figure 5C). The appearance of the new band at 1109 cm^{-1} corresponds to C−O stretching (νCO) with the metal ion (Fe^{3+}/Cu^{2+}) bonded to the L-DOPA catechol oxygen.[47] Overall, photophysical studies, mass and IR analyses further confirmed the formation of metallosupramolecular aggregates via strong M-O chelation.

To investigate the fluorescence quenching mechanism of **1** in the presence of Fe^{3+} and Cu^{2+}, we further carried out the time-correlated single photon counting (TCSPC) experiments with a nanosecond excitation (Figure 5D). TCSPC data displayed quite similar biexponential decay patterns of **1** in the absence and presence of metal ions in aqueous CTAB media. The lifetime values for **1** in CTAB solutions (1.27 ns 63% and 5.44 ns 41%) were almost unaffected upon interaction with Fe^{3+} (1.31 ns 69% and 5.1 ns 35%) and Cu^{2+} (1.38 ns 55% and 5.4 ns 42%) metal ions. The unaffected lifetimes and decay patterns clearly indicating the occurrence of static type quenching via displacement of **1** from CTAB-micelle to nonfluorescent ground state with stable [**1**+Fe^{3+}/Cu^{2+}] metallosupramolecular aggregates (State-IV in Figure 4C). It is reasonable to assume a type of complexation between **1** and metal ion (Fe^{3+}/Cu^{2+}) in the ground state and such a complexation efficiently facilitated the reassembly of **1** in CTAB micellar aqueous solution.

Next, we explored disassembly of the metallosuparamolecular aggregate (State-IV) of **1** in a reversible manner by engaging a metal chelator. In the literature, it has been established that anions, amino acids and other related compounds are capable of taking out or making a ternary complex from/with a ligand−metal system.[46,47] To test this concept, various kinds of anions and neutral, metal ion receptors such as amino acids, ethylenediaminetetraacetic acid (EDTA) and diethylenetriamine pentaacetic acid (DTPA) were employed in our investigations. Fluorometric study of **1** in State-IV indicated

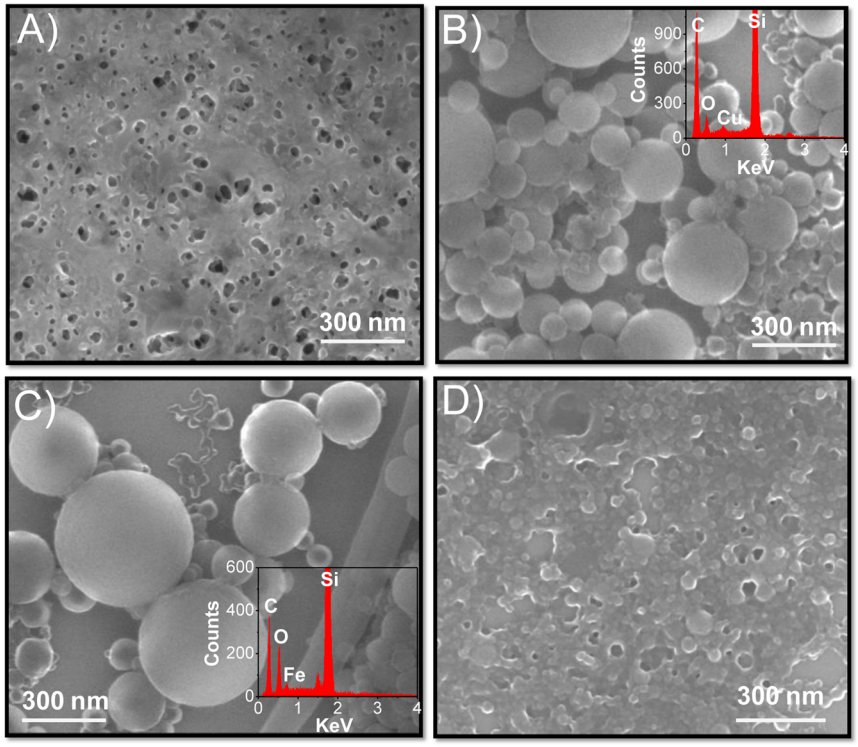

Figure 7. FESEM micrographs of (A) **1**, (B) **1**+Cu^{2+}, (C) **1**+Fe^{3+} and (D) **1**+Cu^{2+}+DTPA. Insets in (B) and (C) EDAX chemical composition mapping graph on corresponding nanospheres.

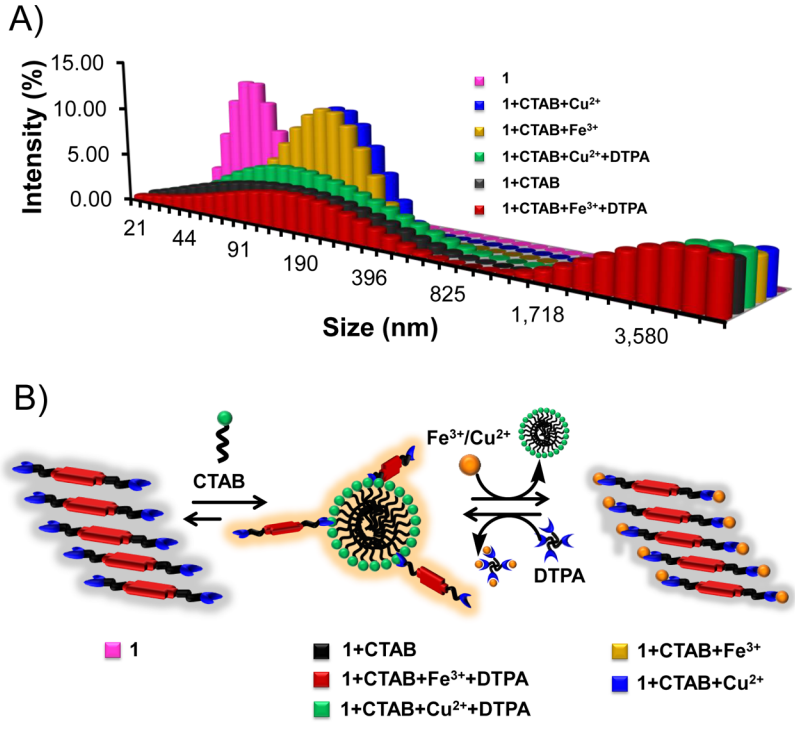

Figure 8. (A) Dynamic light scattering (DLS) size distribution graph. (B) Schematic representation of assembly−disassembly modulation of **1** observed from DLS studies (A).

no change in the quenched fluorescence in the presence of various anions and amino acids even at six times higher concentrations indicating these ligands are unable to disassemble perylene core of **1** in State-IV. Further, our study was continued with well- known metal ion chelators such as EDTA and DTPA. We found that EDTA, even at 100 μM concentrations could hardly alter the metal ions (Fe^{3+} and Cu^{2+}) mediated quenched fluorescence of **1** (State-IV). Interestingly, significant fluorescence enhancement was observed upon treating State-IV (**1**+Fe^{3+}/Cu^{2+}) with DTPA as shown in Figure 6. Addition of DTPA (0−50 μM) into the solution of [**1**+Fe^{3+}/Cu^{2+}] in the micelle media of CTAB

dx.doi.org/10.1021/am5063844 | ACS Appl. Mater. Interfaces 2014, 6, 21369−21379

significantly altered the quenched fluorescence of **1**. A turn-on fluorescence signal with a yellow emission color under green laser was detected (Figure 6A,B inset). This fluorescence recovery was found to be almost 98% for DTPA concentration of 50 μM. The quantitative fluorescence recovery is attributed to efficient metal ion (Fe^{3+}/Cu^{2+}) sequestration by DTPA in the miceller media. This was further confirmed by the changes in absorption spectra of [**1**+Fe^{3+}/Cu^{2+}] in the presence of DTPA (0−50 μM), in the miceller media as shown in Figure 6C,D. Absorption spectra of [**1**+Fe^{3+}] and [**1**+Cu^{2+}] displayed an increase in 0−0 and decrease in 0−1 transition bands upon addition of DTPA. The increase or decrease in transition bands continued until the ratio of 0−0 and 0−1 bands reached closed to 1.6, which is similar to the normal Franck−Condon progressions for disassembled **1** in CTAB solution. Therefore, the absorption spectra with 530, 492, 460 and 430 nm bands are considered as characteristic of the well-resolved vibronic structures corresponding to the 0−0, 0−1, 0−2 and 0−3 transitions, respectively. Interestingly, DTPA treated metallosupramolecular aggregates (State-IV) showed absorption spectral changes similar to absorption patterns observed for **1** in CTAB micellar aqueous medium (State-III) and just reverse as compared to [**1**+Fe^{3+}] and [**1**+Cu^{2+}] (Figure 4A,B). Overall, the strong metal chelator DTPA was able to sequestrate the metal ion (Fe^{3+}/Cu^{2+}) in a competitive environment of metal ion bound **1** in CTAB miceller media. This resulted in the recovery of disassembled or molecularly dissolved State-III of **1** from State-IV, which clearly reflected in the change of spectral features in both absorption and emission studies (Figure 6E).

To visualize the effect of assembly modulation of **1**, we performed field emission scanning electron microscopy (FESEM) studies by drop casting the aqueous solutions onto Si wafers followed by vacuum drying under room temperature. PDI **1** alone formed a uniform film with a porous nature (Figure 7A). Interestingly, complexation of metal ions (Cu^{2+} or Fe^{3+}) transformed the morphology into nanospheres 50−300 nm in diameter (Figure 7B,C). The observed nanospheres, as a consequence of metallosupramolecular aggregates, were further validated by energy dispersive X-ray analysis (EDAX). An EDAX chemical composition mapping graph on corresponding nanospheres indicated the presence of metals (Cu and Fe) along with carbon (C) and oxygen (O), as shown in Figure 7B,C (insets). Further, the metal mediated metallosupramolecular nanospheres could be reverted back to film state by the addition of metal scavenger DTPA as shown in Figure 7D. Therefore, in addition to photophysical studies the reversible assembly−disassembly of **1** was clearly established by the microscopy studies.

Dynamic light scattering (DLS) experiments further supported the assembly modulation of **1** (Figure 8A). PDI **1** alone (State-II) showed the presence of smaller aggregates with a mean size of 44 nm. Whereas addition of CTAB transformed the smaller aggregates of **1** into two distinct aggregates with mean sizes of 90 and 4000 nm, which suggested the formation of State-III. Further, addition of metal ions (Cu^{2+} or Fe^{3+}) into **1** under miceller conditions of CTAB led to the appearance of aggregates in the region of 50−300 nm along with the a small fraction centered around 4000 nm, thus corresponding to State-IV. However, upon addition of metal chelator/scavenger DTPA, a significant decrease in the number of aggregates in the region 50−300 nm was observed and the size distribution was found to be similar to that of State-III (**1**+CTAB). Overall, in agreement with photophysical and microscopy studies, DLS data confirmed the predominant assembled state of **1** in water, which could be disrupted into a disassembled form in the miceller conditions of CTAB. Addition of metal ions (Cu^{2+}/Fe^{3+}) led to the assembled state as consequence of formation of metallosupramolecular aggregates of **1**. Again, addition of DTPA into metallosupramolecular aggregates of [**1**/CTAB/Fe^{3+}] and [**1**/CTAB/Cu^{2+}] restored the disassembled state of **1**, as shown in Figure 8B.

In solution, molecular self-assemblies are considered to be more sensitive toward their environment, nature of solvents, pH of solution, guest molecules, among other factors. Guest molecules may either stimulate or suppress the molecular self-assemblies. Conversely, sometimes guest molecules may not influence the molecular assemblies and disassemblies due to lack of specific interactions. However, in the present study, we were able to modulate the molecular self-assembly of PDI derivative **1** in aqueous media (assembled state, State-II) by means of host−guest interactions provided by micellar structures of CTAB (disassembled state, State-III), metal ion (Fe^{3+} and Cu^{2+}) interactions (assembled state, State-IV) and metal ion sequestration agent DTPA (disassembled state, State-III).

4. CONCLUSION

In conclusion, we developed the amphiphilic L-DOPA functionalized PDI derivative **1** and investigated photophysical properties to achieve its disassembled (molecularly dissolved) state in aqueous media using cationic micellar conditions. Assembly−disassembly modulation of **1** was established as a supramolecular fluorescent probe (switch off−on probe) for metal ions Fe^{3+} and Cu^{2+} in the miceller media of cationic surfactant solution. Our study demonstrated that the complementary electrostatic interactions of cationic surfactant (CTAB) and L-DOPA led to a well-structured absorption spectra and a dramatic increase in the yellow fluorescence of PDI **1** in aqueous medium. These spectral properties were similar to the parent disassembled PDI chromophore **1** in DMSO. Anionic and neutral surfactants could hardly modify the assembled state of **1** in aqueous media. This emphasizes the utility of the assembled state of **1** as a selective fluorescent probe for the cationic surfactant (CTAB). Furthermore, **1** serves as a fluorometric probe for Fe^{3+} and Cu^{2+} by means of fluorescence switch off state due to the formation of metallosupramolecular assemblies. Interestingly, DTPA could sequestrate Fe^{3+}/Cu^{2+} from metallosupramolecular assemblies and transform **1** into a disassembly state, which corresponds to fluorescence switch on state. The assembly−disassembly modulation of **1** was extensively studied using IR, ESI-MS analysis, FESEM and DLS techniques. Overall, the fluorescence switch off−on probe (**1**) based on assembly modulation offers practical utility for analytes detection and understanding of reversible assembly and disassembly of PDI derivatives by means of tunable host−guest interactions in aqueous media.

■ ASSOCIATED CONTENT

Ⓢ Supporting Information

Experimental methods, photophysical studies of **1** upon increasing addition SDS in water, photophysical studies of **1** upon increasing addition Triton X-100 in water, fluorescence emission studies of [**1**+CTAB+Fe^{3+}] in presence of various anions, amino acids and metal chelators, fluorescence emission studies of [**1**+CTAB+Cu^{2+}] in presence of various anions, amino acids and metal chelators, pH dependent fluorescence

response studies and ^{1}HNMR and ^{13}C NMR spectra of **1**. This material is available free of charge via the Internet at http://pubs.acs.org.

AUTHOR INFORMATION

Corresponding Author

*T. Govindaraju. E-mail: tgraju@jncasr.ac.in.

Author Contributions

‡A.K.D. and M.P. contributed equally. The paper was written through contributions of all authors. All authors have given approval to the final version of the paper.

Notes

The authors declare no competing financial interest.

ACKNOWLEDGMENTS

The authors thank Prof. C. N. R. Rao for constant support and encouragement, JNCASR, research grants from the Council of Scientific Industrial and Research (CSIR) [02(0128)/13/EMR-II], Department of Biotechnology (DBT)-Innovative Young Biotechnologist Award (IYBA) (BT/03/IYBA/2010), New Delhi, India, Sheikh Saqr Laboratory (SSL), ICMS-JNCASR for awarding Sheikh Saqr Career Award Fellowship to T.G. and CSIR Research Associate fellowship to A.K.D.

REFERENCES

(1) Wuerthner, F. Perylene Bisimide Dyes As Versatile Building Blocks for Functional Supramolecular Architectures. *Chem. Commun.* **2004**, *14*, 1564−1579.

(2) Avinash, M. B.; Govindaraju, T. Amino Acid Derivatized Arylenediimides: A Versatile Modular Approach for Functional Molecular Materials. *Adv. Mater.* **2012**, *24*, 3905−3922.

(3) Che, Y.; Yang, X.; Zang, L. Ultraselective Fluorescent Sensing of Hg^{2+} through Metal Coordinationinduced Molecular Aggregation. *Chem. Commun.* **2008**, *12*, 1413−1415.

(4) Peneva, K.; Mihov, G.; Herrmann, A.; Zarrabi, N.; Börsch, M.; Duncan, T. M.; Müllen, K. Exploiting the Nitrilotriacetic Acid Moiety for Biolabeling with Ultrastable Perylene Dyes. *J. Am. Chem. Soc.* **2008**, *130*, 5398−5399.

(5) Chen, X.; Jou, M. J.; Yoon, J. An "Off-On" Type UTP/UDP Selective Fluorescent Probe and Its Application to Monitor Glycosylation Process. *Org. Lett.* **2009**, *11*, 2181−2184.

(6) Wang, B.; Yu, C. Fluorescence Turn-On Detection of a Protein Through the Reduced Aggregation of a Perylene Probe. *Angew. Chem., Int. Ed.* **2010**, *49*, 1485−1488.

(7) Szekle, H.; Schübel, S.; Harenberg, J.; Krämer, R. A. Fluorescent Probe for the Quantification of Heparin in Clinical Samples with Minimal Matrix Interference. *Chem. Commun.* **2010**, *46*, 1667−1669.

(8) Sadrai, M.; Bird, G. R. A New Laser Dye with Potential for High Stability and a Broad Band of Lasing Sction: Perylene-3,4,9,10-tetracarboxylic Acid-Bis-N,N′(2′,6′-xylidyl)diimide. *Opt. Commun.* **1984**, *51*, 62−64.

(9) Ford, W. E.; Kamat, P. V. Photochemistry of 3,4,9,1O-Perylenetetracarboxylic Dianhydride Dyes. 3. Singlet and Triplet Excited-State Properties of the Bis(2,5-di-tert-butylphenyl)imide Derivative. *J. Phys. Chem.* **1987**, *91*, 6373−6380.

(10) Schmidt-Mende, L.; Fechtenkotter, A.; Müllen, K.; Moons, E.; Friend, R. H.; MacKenzie, J. D. Self-Organized Discotic Liquid Crystals for High-Efficiency Organic Photovoltaics. *Science* **2001**, *293*, 1119−1122.

(11) Li, J. L.; Dierschke, F.; Wu, J. S.; Grimsdale, A. C.; Mullen, K. Poly(2,7-carbazole) and Perylene Tetracarboxydiimide: A Promising Donor/Acceptor Pair for Polymer Solar Cells. *J. Mater. Chem.* **2006**, *16*, 96−100.

(12) Ye, T.; Singh, R.; Butt, H.-J.; Floudas, G.; Keivanidis, P. E. Effect of Local and Global Structural Order on the Performance of Perylene Diimide Excimeric Solar Cells. *ACS Appl. Mater. Interfaces* **2013**, *5*, 11844−11857.

(13) Singh, R.; Mróz, M. M.; Di Fonzo, F.; Cabanillas-Gonzalez, J.; Marchi, E.; Bergamini, G.; Müllen, K.; Jacob, J.; Keivanidis, P. E. Improving the Layer Morphology of Solution-Processed Perylene Diimide Organic Solar Cells with the Use of a Polymeric Interlayer. *Org. Photonics Photovoltaics* **2013**, *1*, 24−38.

(14) Liu, Y.; Wang, N.; Li, Y.; Liu, H.; Li, Y.; Xiao, J.; Xu, X.; Huang, C.; Cui, S.; Zhu, D. A New Class of Conjugated Polyacetylenes Having Perylene Bisimide Units and Pendant Fullerene or Porphyrin Groups. *Macromolecules* **2005**, *38*, 4880−4887.

(15) Feng, X.; An, Y.; Yao, Z.; Li, C.; Shi, G. A Turn-on Fluorescent Sensor for Pyrophosphate Based on the Disassembly of Cu^{2+}-Mediated Perylene Diimide Aggregates. *ACS Appl. Mater. Interfaces* **2012**, *4*, 614−618.

(16) Liu, X.; Zhang, N.; Zhou, J.; Chang, T.; Fang, C.; Shangguan, D. A Turn-on Fluorescent Sensor for Zinc and Cadmium Ions Based on Perylene Tetracarboxylic Diimide. *Analyst* **2013**, *138*, 901−906.

(17) Bo, F.; Gao, B.; Duan, W.; Li, H.; Liu, H.; Bai, Q. Assembly−Disassembly Driven "Off−On" Fluorescent Perylene Bisimide Probes for Detecting and Tracking of Proteins in Living Cells. *RSC Adv.* **2013**, *3*, 17007−17010.

(18) Tang, T.; Peneva, K.; Mullen, K.; Webber, S. E. Photophysics of Water Soluble Perylene Diimides in Surfactant Solution. *J. Phys. Chem. A* **2007**, *111*, 10609−10614.

(19) Zheng, Y.; Long, H.; Schatz, G. C.; Lewis, F. D. Duplex and Hairpin Dimer Structures for Perylene Diimide−Oligonucleotide Conjugates. *Chem. Commun.* **2005**, *38*, 4795−4797.

(20) Jones, B. A.; Ahrens, M. J.; Yoon, M. H.; Facchetti, A.; Marks, T. J.; Wasielewski, M. R. High-Mobility Air-Stable n-Type Semiconductors with Processing Versatility: Dicyanoperylene-3,4:9,10-Bis(dicarboximides). *Angew. Chem., Int. Ed.* **2004**, *43*, 6363−6366.

(21) Zhao, C.; Zhang, Y.; Li, R.; Li, X.; Jiang, J. Di(alkoxy)- and Di(alkylthio)-Substituted Perylene-3,4;9,10-tetracarboxy Diimides with Tunable Electrochemical and Photophysical Properties. *J. Org. Chem.* **2007**, *72*, 2402−2410.

(22) Wang, H.; Wang, D.; Wang, Q.; Li, X.; Schalley, C. A. Nickel(II) and Iron(III) Selective Off-On-type Fluorescence Probes Based on Perylene tetracarboxylic diimide. *Org. Biomol. Chem.* **2010**, *8*, 1017−1026.

(23) He, X.; Liu, H.; Li, Y.; Wang, S.; Li, Y.; Wang, N.; Xiao, J.; Xu, X.; Zhu, D. Gold Nanoparticle-based Fluorometric and Colorimetric Sensing of Copper(II) Ions. *Adv. Mater.* **2005**, *17*, 2811−2815.

(24) Che, Y.; Yang, X.; Zang, L. Ultraselective Fluorescent Sensing of Hg^{2+} through Metal Coordination-Induced Molecular Aggregation. *Chem. Commun.* **2008**, 1413−1415.

(25) Ehli, C.; Oelsner, C.; Guldi, D. M.; Mateo-Alonso, A.; Prato, M.; Schmidt, C.; Backes, C.; Hauke, F.; Hirsch, A. Manipulating Single-Wall Carbon Nanotubes by Chemical Doping and Charge Transfer with Perylene Dyes. *Nat. Chem.* **2009**, *1*, 243−249.

(26) Backes, C.; Schmidt, C. D.; Hauke, F.; Bçttcher, C.; Hirsch, A. High Population of Individualized SWCNTs Through the Adsorption of Water-Soluble Perylenes. *J. Am. Chem. Soc.* **2009**, *131*, 2172−2184.

(27) Baram, J.; Shirman, E.; Ben-Shitrit, N.; Ustinov, A.; Weissman, H.; Pinkas, I.; Wolf, S. G.; Rybtchinski, B. Control Over Self-Assembly through Reversible Charging of the Aromatic Building Blocks in Photofunctional Supramolecular Fibers. *J. Am. Chem. Soc.* **2008**, *130*, 14966−14967.

(28) Zhang, X.; Rehm, S.; Safont-Sempere, M. M.; Wurthner, F. Vesicular Perylene Dye Nanocapsules as Supramolecular Fluorescent pH Sensor Systems. *Nat. Chem.* **2009**, *1*, 623−629.

(29) Biedermann, F.; Elmalem, E.; Ghosh, I.; Nau, W. M.; Scherman, O. A. Strongly Fluorescent, Switchable Perylene Bis(diimide) Host-Guest Complexes with Cucurbit[8]uril in Water. *Angew. Chem., Int. Ed.* **2012**, *51*, 7739−7743.

(30) Maity, D.; Manna, A. K.; Karthigeyan, D.; Kundu, T. K.; Pati, S. K.; Govindaraju, T. Visible-near Infrared and Fluorescent Copper Sensors Based on Julolidine Conjugates: Selective Detection and

Fluorescence Imaging in Living Cells. *Chem.—Eur. J.* **2011**, *17*, 11152−11161.
(31) Maity, D.; Govindaraju, T. Highly Selective Visible and near-IR Sensing of Cu(II) Based on Thiourea−Salicylaldehyde Coordination in Aqueous Media. *Chem.—Eur. J.* **2011**, *17*, 1410−1414.
(32) Narayanaswamy, N.; Govindaraju, T. Aldazine-based Colorimetric Sensors for Cu(II) and Fe(III). *Sens. Actuators, B* **2012**, *161*, 304−310.
(33) Sahoo, S. K.; Sharma, D.; Bera, R. K.; Crisponi, G.; Callan, J. F. Iron(III) Selective Molecular and Supramolecular Fluorescent Probes. *Chem. Soc. Rev.* **2012**, *41*, 7195−7227.
(34) Maitya, D.; Karthigeyan, D.; Kundu, T. K.; Govindaraju, T. FRET-based Rational Strategy for Ratiometric Detection of Cu(II) and Live Cell Imaging. *Sens. Actuators, B* **2013**, *162*, 831−837.
(35) Barnham, K. J.; Bush, A. I. Biological Metals and Metal-Targeting Compounds in Major Neurodegenerative Diseases. *Chem. Soc. Rev.* **2014**, *43*, 6727−6749.
(36) Lemouchi, C.; Simonov, S.; Zorina, L.; Gautier, C.; Hudhomme, P.; Batail, P. Amino Acid Derivatives of Perylenediimide and Their N-HO Peptide Bond Dipoles-Templated Solid State Assembly into Stacks. *Org. Biomol. Chem.* **2011**, *9*, 8096−8101.
(37) Ponnuswamy, N.; Pantos, G. D.; Smulders, M. M. J.; Sanders, J. K. M. Thermodynamics of Supramolecular Naphthalenediimide Nanotube Formation: The Influence of Solvents, Side Chains, and Guest Templates. *J. Am. Chem. Soc.* **2012**, *134*, 566−573.
(38) Pandeeswar, M.; Avinash, M. B.; Govindaraju, T. Chiral Transcription and Retentive Helical Memory: Probing Peptide Auxiliaries Appended with Naphthalenediimides for Their One-Dimensional Molecular Organization. *Chem.—Eur. J.* **2012**, *18*, 4818−4822.
(39) Pandeeswar, M.; Govindaraju, T. Green-Fluorescent Naphthalene Diimide: Conducting Layered Hierarchical 2D Nanosheets and Reversible Probe for Detection of Aromatic Solvents. *RSC Adv.* **2013**, *3*, 11459−11462.
(40) Pandeeswar, M.; Khare, H.; Ramakumar, S.; Govindaraju, T. Biomimetic Molecular Organization of Naphthalene Diimide in the Solid State: Tunable (Chiro-) Optical, Viscoelastic and Nanoscale Properties. *RSC Adv.* **2014**, *4*, 20154−20163.
(41) Bai, S.; Debnath, S.; Javid, N.; Frederix, P. W. J. M.; Fleming, S.; Pappas, C.; Ulijn, R. V. Differential Self-Assembly and Tunable Emission of Aromatic Peptide Bola-Amphiphiles Containing Perylene Bisimide in Polar Solvents Including Water. *Langmuir* **2014**, *30*, 7576−7584.
(42) Li, A. D. Q.; Wang, W.; Wang, L.-Q. Folding versus Self-Assembling. *Chem.—Eur. J.* **2003**, *9*, 4594−4601.
(43) Würthner, F.; Chen, Z.; Dehm, V.; Stepanenko, V. One-Dimensional Luminescent Nanoaggregates of Perylene Bisimides. *Chem. Commun.* **2006**, *11*, 1188−1190.
(44) García, C. R.; Angelé-Martínez, C.; Wilkes, J. A.; Wang, H. C.; Battin, E. E.; Brumaghim, J. L. Prevention of Iron- and Copper-Mediated DNA Damage by Catecholamine and Amino Acid Neurotransmitters, L-DOPA, and Curcumin: Metal Binding as a General Antioxidant Mechanism. *Dalton Trans.* **2012**, *41*, 6458−6467.
(45) Mialane, P.; Anxolabehere-Mallart, E.; Blondin, G.; Nivorojkine, A.; Guilhem, J.; Tchertanova, L.; Cesario, M.; Ravi, N.; Bominaar, E.; Girerd, J.-J.; Munck, E. Structure and Electronic properties of (N,N-Bis(4-methyl-6-tert-butyl-2-methyl-phenolato)-N,N-bismethyl-1,2-diaminoethane FeIII (DBSQ). Spectroelectrochemical Study of the Red-Ox Properties. Relevance to Intradiol Catechol Dioxygenases. *Inorg. Chim. Acta* **1997**, *263*, 367−378.
(46) Saikia, G.; Dwivedi, A. K.; Iyer, P. K. Development of Solution, Film and Membrane based Fluorescent Sensor for the Detection of Fluoride Anions from Water. *Anal. Methods* **2012**, *4*, 3180−3186.
(47) Dwivedi, A. K.; Saikia, G.; Iyer, P. K. Aqueous Polyfluorene Probe for the Detection and Estimation of Fe^{3+} and Inorganic Phosphate in Blood Serum. *J. Mater. Chem.* **2011**, *21*, 2502−2507.